Research Advances

Cenozoic Exhumation History of the East Kunlun Orogenic Belt Constrained by Apatite Fission-Track Thermochronology

YANG Wei[1, 2], XIA Guoqing[1, 3, *], WU Chihua[4] and YI Haisheng[1, 3]

1 *Institute of Sedimentary Geology, Chengdu University of Technology, Chengdu 610059, Sichuan, China*
2 *282 Brigade of Sichuan Nuclear Geology, Deyang 618000, Sichuan, China*
3 *State Key Laboratory of Oil & Gas Reservoir Geology and Exploitation, Chengdu 610059, Sichuan, China*
4 *School of Marine Sciences, Sun Yat-sen University, Zhuhai 519082, Guangdong, China*

Objective

The East Kunlun Orogenic belt constitutes the first marked change in the topographic reliefs north of the Qinghai–Tibet Plateau. The Cenozoic tectonic evolution of this orogenic belt is crucial for understanding the remote deformational effects of the Eurasian plate collision and the migration track at the northern margin of the plateau. However, when and how the uplift occurred remains controversial (Wang Chengshan et al., 2008; Yin An et al., 2007; Yi Haisheng et al., 2008). In this study, we report detrital apatite fission track (ATF) results from Cenozoic strata of the Changweitai section at the southern margin of the Qaidam Basin in order to elucidate the tectonic evolutionary history of the East Kunlun Orogenic Belt.

Methods

A total of 16 Cenozoic sandstone samples were dated with the AFT method from Changweitai section (N 37°48′20.9″, E 91°23′ 12.8″). All samples were measured by using the external detector method, and a zeta calibration factor determined from the Fish Canyon and Durango of ζ=352.4±29 Ma. CN5 glass was used as a dosimeter. Spontaneous fission tracks were etched with 5.5% HNO_3 for 20 s at 20°C, and evoked track etching was conducted in 40%HF for 40 minutes at 20° C. Fission tracks were counted using an OLYMPUS microscope at a magnification of 1000. At least 100 grains per sample were dated independently to obtain statistically robust results when the observed grain-age distribution is decomposed into major grain-age components or peaks.

Results

Binomial peak fitting reveal that each sample contains three or four main AFT-age peaks, except for the sample CNY1-59L from the Shangyoushashan Formation with two peaks. The youngest (P1), second youngest (P2), and third (P3) population peak ages have distinct similar trends (Fig. 1). The P1 ages of three samples from Xiaganchaigou Fm. and sample CNG2-41L from Shanggancgou Fm. are significantly younger than depositional ages, and expressed as a progressive decrease within the older sediments, suggesting that the apatite grains may have been partially reset during their burial process. For unannealed apatite

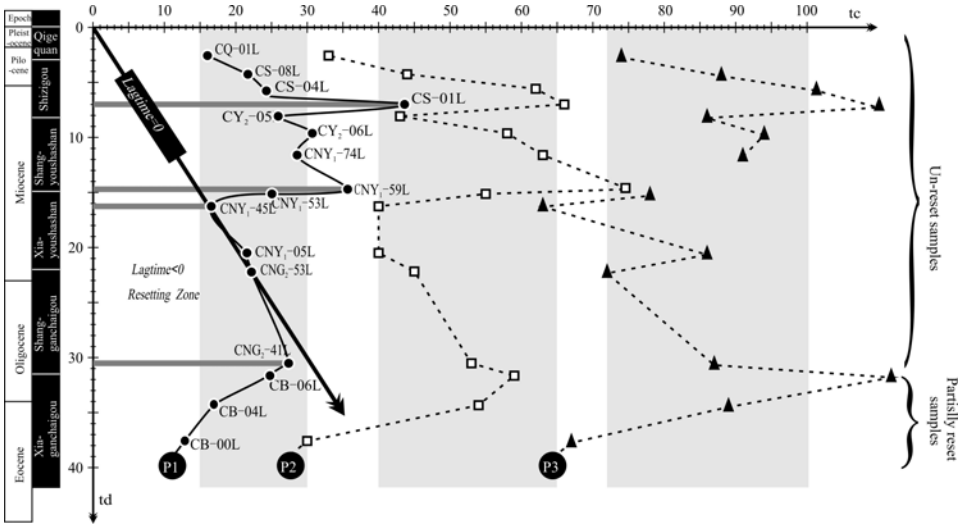

Fig. 1. Plot of detrital AFT population ages for samples from the Changweitai section. P1, P2 and P3 represent the youngest, second youngest, and third population peak ages, respectively.

* Corresponding author. E-mail: xiaguoqing2012@cdut.cn

fission track age, peaks P1, P2, and P3 range from 16 to 35.6 Ma, 39.8 to 75 Ma, and 63.6 to 109.6 Ma, respectively, and are concentrated around 15–30, 40–65, and 72–100 Ma, respectively (Fig. 1; Appendix 1). The fourth peak, P4, mainly indicates ages between 118.8 and 216.1 Ma and concentrate around 120–150 Ma. These age distributions reflect periods of orogenic uplift events in the source region. Moreover, the un-reset samples with depositional ages older than 16.2 Ma (CNG2-41L–CNY1-45L) show a normal AFT age sequences with gradually decreasing population ages. During 16.2–14.9 Ma (CNY1-45L–CNY1-59L), the component ages of P1 and P2 (no P3 at sample CNY1-59L) sharply increase, forming a reverse detrital AFT age sequence. After ~14.9 Ma, the component ages progressively decrease except for a sharply pulse in the component ages at ~7.2 Ma (CS-01L), but then it rapidly trips back to the identical development path (Fig. 1).

Conclusions

Apatite fission-track analysis revealed four periods of regional tectonic-thermal activity in the east Kunlun Mountain region. These events began in the Mid–Late Mesozoic (150–120 Ma), and recurred at 100–72, 65–40, and 30–15 Ma. In addition, two normal AFT sequences occur at ~33.4–16.2 Ma and ~14.9–2.5 Ma, implying two continuously stable uplifting processes in the east Kunlun region respectively. Furthermore, there were two significant reverse AFT sequences at ~16.2–14.9 Ma and ~7.2 Ma, representative of provenance variation or tectonic activity.

Acknowledgements

This work was financially supported by the National Natural Science Foundation of China (grants No. 41402099 and No. 40972084).

References

Wang Chengshan, Zhao Xixi, Liu Zhifei, Lippert Peter C, Graham Stephan A, Coe Stephan A, Yi Haisheng, Zhu Lidong, Liu Shun and Li Yalin, 2008. Constraints on the early uplift history of the Tibetan Plateau. *Proceedings of the National Academy of Sciences of the United States of America*, 105(13): 4987.

Yin An, Dang Yuqi, Zhang Min, Mcrivette Michael W, Burgess W Paul and Chen Xuanhua, 2007. Cenozoic tectonic evolution of Qaidam Basin and its surrounding regions (part 2): wedge tectonics in southern Qaidam Basin and the Eastern Kunlun Range. *The Geological Society of America*, 433: 369–390.

Yi Haisheng, Wang Chengshan, Shi Zhiqiang, Lin Jinhui and Zhu Lidong, 2008. Early uplift history of the Tibetan Plateau: records from paleocurrents and paleodrainage in the Hoh Xil Basin: *Acta Geologica Sinica* (English Edition), 82(1): 206–213.

Appendix 1 Apatite fission track data from the Changweitai section

Sample	Dep/age (Ma)	$RHO_D(N_D)$ ($\times10^5cm^{-2}$)	$\rho_s(N_s)$ ($\times10^5cm^{-2}$)	$\rho_i(N_i)$ ($\times10^5cm^{-2}$)	U Con. (ppm)	Age range (Ma)	$P(\chi^2)$/%	P1	P2	P3	P4
Qigequan Formation											
CQ-01L	2.5	10.1(2521)	2.339(1588)	13.88(9425)	17.2	6–111.5	0	16±2.4 (21%)	33.2±2.5(64%)	74.5±5.8(15%)	—
Shizigou Formation											
CS-08L	4.2	10.1(2501)	3.987(2175)	14.37(7838)	17.8	8.8–254.9	0	21.6±2.2 (25%)	44.1±3.4 (39%)	88.5±9.8(33%)	—
CS-04L	5.9	9.76(2442)	6.01(4027)	12.52(8386)	16	14.4–309	0	24.7±2 (16%)	62.2±5.1 (24%)	102.5±8.1(41%)	150.6±14(19%)
CS-01L	7.2	9.46(2382)	5.46(3567)	12.46(8123)	16.5	16.2–249.5	0	41.8±4.5 (19)	66.3±6.7 (31%)	109.6±6.1(50%)	—
CY2-05L	8.1	9.29(2323)	5.191(3187)	12.88(7908)	17.3	18.8–237.6	0	25.9±3.4 (11%)	43.2±3.6 (31%)	86±4.6(46%)	144.4±12(12%)
Shangyoushashan Formation											
CY2-06L	9.4	9.21(2303)	4.999(3542)	11.98(8487)	16.3	17.8–232.9	0	30.7±2.2 (23%)	57.6±4.5 (27%)	94±6.2(38%)	142.1±12(12%)
CNY1-74L	11.2	8.89(2224)	6.475(2980)	14.06(6471)	19.8	13.7–416.4	0	28.4±3.8 (7%)	63.1±9.2 (57%)	91.1±29(36%)	—
CNY1-59L	14.9	8.58(2145)	4.03(1934)	11.53(5535)	16.8	16.2–210.6	0	35.6±2.8 (47%)	75±5.1 (53%)	—	—
Xiaoyoushashan Formation											
CNY1-53L	15.8	8.5(2125)	3.79(2768)	10.37(7561)	15.3	10.6–149.8	0	24.8±2.1 (21%)	54.6±5.4 (44%)	78.4±8.2(33%)	120.6±28(2%)
CNY1-45L	16.2	8.42(2105)	7.567(5062)	15.12(10117)	22.4	11.9–215.4	0	16.5±3.3(4%)	40.1±4.3 (15%)	63.6±4(47%)	106.9±5(34%)
CNY1-05L	20.6	7.79(1947)	4.77(3136)	15.07(9893)	24.2	10.7–225.3	0	21.5±1.9(19%)	39.8±2.3(49%)	85.7±45(39%)	216.1±51(2%)
Shangganchaigou Formation											
CNG2-53L	22.5	7.71(1927)	6.437(4317)	12.86(8626)	20.9	7.6–203.4	0	22.9±3(6%)	45.1±3.1(24%)	72.1±5.4(32%)	118.8±6(38%)
CNG2-41L	33.4	10(2500)	5.619(3172)	14.63(8258)	18.3	18.6–221.9	0	27.2±5(7%)	53.1±3.5(44%)	87.1±5.6(38%)	127.2±14(11%)
Xiaganchaigou Formation											
CB-06L	36.4	9.81(2452)	5.739(3934)	17.52(12010)	22.3	10.8–190.9	0	24.5±1.3(23%)	58.7±3(45%)	116.2±5.9(32%)	—
CB-04L	37.4	9.71(2428)	3.879(2205)	15.78(8972)	20.3	5.4–223.5	0	16.9±1(15%)	54.1±3.5(39%)	89.2±8.7(10%)	—
CB-00L	40	9.62(2405)	2.874(2186)	13.84(10525)	18	7.3–129.5	0	12.8±2(11%)	30.3±1.5(60%)	67.2±3.8(29%)	—

Notes: RHO_D, induced fission track density of dosimeter glass CN5; N_D, number of induced fission tracks of dosimeter glass CN5; ρ_s, spontaneous track density; N_s, number of fission tracks counted; ρ_i, induced track density in external detector (muscovite); N_i, number of induced tracks counted; U Con., uranium concentration; P1, P2, P3 and P4, peak ages were determined with BINOMFITand given with 95% confidence interval. Depositional age calculated based on the biostratigraphy and magnetostratigraphy of Cenozoic series and adjusted by average deposition rate of stratigraphic systems.